



Discovery of small molecule guanylyl cyclase A receptor positive allosteric modulators

S. Jeson Sangaralingham^{a,b,1}, Kanupriya Whig^c, Satyamaheshwar Peddibhotla^{c,d}, R. Jason Kirby^c, Hampton E. Sessions^c, Patrick R. Maloney^c, Paul M. Hershberger^c, Heather Mose-Yates^d, Becky L. Hood^c, Stefan Vasile^c, Shuchong Pan^a, Ye Zheng^a, Siobhan Malany^{c,d,1,2}, and John C. Burnett Jr.^{a,b,1,2}

^aCardiorenal Research Laboratory, Department of Cardiovascular Medicine, Mayo Clinic, Rochester, MN 55905; ^bDepartment of Physiology and Biomedical Engineering, Mayo Clinic, Rochester, MN 55905; ^cChemical Genomics Center, Sanford Burnham Prebys Medical Discovery Institute, La Jolla, CA 92037; and ^dDepartment of Pharmacodynamics, University of Florida, Gainesville, FL 32610

Edited by Joseph A. Beavo, University of Washington School of Medicine, Seattle, WA, and approved October 29, 2021 (received for review June 3, 2021)

The particulate guanylyl cyclase A receptor (GC-A), via activation by its endogenous ligands atrial natriuretic peptide (ANP) and b-type natriuretic peptide (BNP), possesses beneficial biological properties such as blood pressure regulation, natriuresis, suppression of adverse remodeling, inhibition of the renin-angiotensin-aldosterone system, and favorable metabolic actions through the generation of its second messenger cyclic guanosine monophosphate (cGMP). Thus, the GC-A represents an important molecular therapeutic target for cardiovascular disease and its associated risk factors. However, a small molecule that is orally bioavailable and directly targets the GC-A to potentiate cGMP has yet to be discovered. Here, we performed a cell-based high-throughput screening campaign of the NIH Molecular Libraries Small Molecule Repository, and we successfully identified small molecule GC-A positive allosteric modulator (PAM) scaffolds. Further medicinal chemistry structure–activity relationship efforts of the lead scaffold resulted in the development of a GC-A PAM, MCUF-651, which enhanced ANP-mediated cGMP generation in human cardiac, renal, and fat cells and inhibited cardiomyocyte hypertrophy *in vitro*. Further, binding analysis confirmed MCUF-651 binds to GC-A and selectively enhances the binding of ANP to GC-A. Moreover, MCUF-651 is orally bioavailable in mice and enhances the ability of endogenous ANP and BNP, found in the plasma of normal subjects and patients with hypertension or heart failure, to generate GC-A–mediated cGMP *ex vivo*. In this work, we report the discovery and development of an oral, small molecule GC-A PAM that holds great potential as a therapeutic for cardiovascular, renal, and metabolic diseases.

particulate guanylyl cyclase A receptor | small molecule | cardiovascular disease | natriuretic peptides

The global burden of cardiovascular diseases (CVDs) and its associated risk factors of hypertension, obesity, and renal dysfunction, all of which are major drivers for premature mortality, are rapidly growing worldwide (1, 2). While drug discovery continues in this area, there remains a high unmet need for novel therapies, especially with innovative molecular targets. Employing native and designer peptides, we and others have established the favorable pleiotropic properties of the particulate guanylyl cyclase A receptor (GC-A) through the generation of its second messenger 3', 5' cyclic guanosine monophosphate (cGMP) (3–6). In response to GC-A activation by the native cardiac hormones atrial natriuretic peptides (ANP) and b-type natriuretic peptides (BNP), such beneficial biological properties include the reduction in blood pressure (BP), natriuresis, suppression of adverse cardiorenal and CV remodeling, inhibition of the renin-angiotensin-aldosterone system (RAAS), and favorable metabolic properties (4–6). Most recently, studies from the PROVE-HF trial have reported that ANP is the predominant natriuretic peptide (NP) increased by sacubitril/valsartan (S/V) and is closely correlated with S/V mediated reverse remodeling, thus supporting a key role for GC-A

activation in the actions of S/V (7). Taken together, these biological properties render the GC-A/cGMP pathway an unprecedented molecular target for CV therapeutics.

Historically, GC-A therapeutics have been dependent on use of synthetic or recombinant peptides forms of ANP and BNP. Specifically, ANP and BNP are both approved for the treatment of acute heart failure (HF) via intravenous (IV) infusion in Japan and the United States, respectively (8, 9). Beyond the need for IV infusion, these ligands have short circulating half-lives due to their rapid enzymatic degradation by neprilysin (NEP) and receptor-mediated clearance through the NP clearance receptor, NPR-C (10). Thus, the development of designer NPs has evolved in an effort to overcome these therapeutic challenges related to short bioavailability and delivery. Indeed,

Significance

The particulate guanylyl cyclase A receptor (GC-A), via its endogenous cardiac-derived hormones atrial natriuretic peptide (ANP) and b-type natriuretic peptide (BNP), plays a pivotal role in maintaining intravascular volume, arterial pressure, cardiovascular structure, function, and, more recently, metabolic homeostasis. As such, therapies to potentiate GC-A signaling via peptide augmentation have yielded promising results in clinical trials. A major breakthrough in GC-A therapeutics would be a small molecule that sensitizes the GC-A receptor to endogenous ANP or BNP, which to date does not exist. Here, we report the development of an orally bioavailable, small molecule positive allosteric modulator of GC-A that exhibits therapeutic activity in human hypertension and heart failure *ex vivo*.

Author contributions: S.J.S., K.W., S. Peddibhotla, R.J.K., H.E.S., P.R.M., P.M.H., B.L.H., S.V., S. Pan, Y.Z., S.M., and J.C.B. designed research; K.W., S. Peddibhotla, R.J.K., H.E.S., P.R.M., P.M.H., H.M.-Y., B.L.H., S.V., S. Pan, Y.Z., and S.M. performed research; S.J.S., S. Peddibhotla, H.E.S., P.R.M., P.M.H., S.M., and J.C.B. contributed new reagents/analytic tools; S.J.S., K.W., S. Peddibhotla, R.J.K., H.E.S., P.R.M., P.M.H., H.M.-Y., B.L.H., S.V., S. Pan, Y.Z., S.M., and J.C.B. analyzed data; and S.J.S., S. Peddibhotla, S. Pan, Y.Z., S.M., and J.C.B. wrote the paper.

Competing interest statement: A patent related to small molecule guanylyl cyclase A receptor enhancers has been filed by the Mayo Foundation for Medical Education and Research and Sanford Burnham Prebys Medical Discovery Institute, of which S.J.S., S. Peddibhotla, P.M.H., H.E.S., P.R.M., S.M., and J.C.B. are listed as inventors, and this technology has been licensed to AlloRock. A patent for the *ex vivo* human therapeutic potency assay has been also filed by the Mayo Foundation for Medical Education and Research, of which S.J.S., Y.Z., and J.C.B. are listed as inventors. This research is being conducted in compliance with Mayo Clinic conflict of interest policies.

This article is a PNAS Direct Submission.

Published under the PNAS license.

¹To whom correspondence may be addressed. Email: sangaralingham.jeson@mayo.edu, smalany@cop.ufl.edu, or burnett.john@mayo.edu.

²S.M. and J.C.B. contributed equally to this work.

This article contains supporting information online at <http://www.pnas.org/lookup/suppl/doi:10.1073/pnas.2109386118/-DCSupplemental>.

Published December 20, 2021.

MANP is a novel ANP analog that possesses greater resistance to NEP degradation compared to ANP and is in clinical trials for resistant hypertension (11, 12). However, as a peptide, MANP must be administered as an injection, similar to that of insulin in diabetes. Hence, the discovery of small molecules, which are noted for favorable oral bioavailability, would represent a major breakthrough in GC-A therapeutics.

Allosteric ligands bind to sites on the receptor that are separate from the orthosteric binding site to which the endogenous ligands, such as ANP and BNP, bind (13). Positive allosteric modulators (PAMs) lack actions when binding to the receptor in the absence of the specific endogenous receptor ligand(s). As such, studies suggest that PAMs have high specificity to receptors (14). Furthermore, in animal models and humans, PAMs operate to physiological and pathophysiological variations in their endogenous ligand hormones and therefore are self-titrating to maximize cell signaling and avoid drug tolerance. To date, no such small molecules have been reported to target the GC-A receptor and to enhance its cGMP-mediated biological effects.

The goal of the current study was to pursue a cell-based high-throughput screening (HTS) campaign to identify small molecule GC-A PAMs using the NIH Molecular Libraries Small Molecule Repository (MLSMR). Here, we report the discovery of small molecule GC-A PAM scaffolds and the identification of a lead molecule, MCUF-651. Moreover, we also designed the following studies to determine the ability of MCUF-651 to 1) augment cGMP in HEK293 cells overexpressing either GC-A or the alternative GC-B receptor so as to establish potency with the endogenous ligands for each receptor and selectivity for GC-A; 2) potentiate cGMP levels, in the presence of ANP, in primary cells naturally expressing GC-A including human renal proximal tubular cells (HRPTCs), human adipocytes (HAs), and human cardiomyocytes (HCM); 3) enhance ANP-mediated anti-hypertrophic actions in HCM; 4) assess the binding of MCUF-651 alone or in the presence of increasing concentrations of ANP/BNP or C-type natriuretic peptide (CNP) to human GC-A and GC-B, respectively; 5) determine the pharmacokinetics (PK) and oral bioavailability in mice; and 6) augment cGMP in a human plasma from normal subjects and patients with hypertension and HF using an *ex vivo* potency assay.

Results

Discovery of Small Molecule GC-A PAM Scaffolds. We successfully screened the NIH MLSMR of 370,620 compounds (Fig. 1) in the presence of a subconcentration (9 pM in 1,536 well screening assay) of ANP to sensitize the HTS toward detection of PAMs and identified 519 hits. Compound concentration-responses in the primary cell-based screening assay and a counter screen assay performed in parental HEK293 cells devoid of expressed GC-A receptor confirmed 273 compounds as potential GC-A enhancers. The hits were confirmed to be devoid of agonist activity in the absence of added ANP when tested in the HEK293-GC-A overexpressed cells, thereby supporting their mode of action as PAMs. These compounds were graded according to activity, structure, and liability as potential pan-assay interference compounds resulting in 62 compounds that met our internal criteria and were available as commercial powders (15). Analogs were furthermore filtered by the absence of any phosphodiesterase 5 (PDE5) inhibitor activity as the PDE5 is involved in the degradation of cGMP, thereby regulating cGMP levels in tissues.

Hit Confirmation Studies. Selective GC-A PAMs from the MLSMR screen were binned according to scaffolds resulting in four chemical scaffolds. Chemical stability, synthetic tractability,

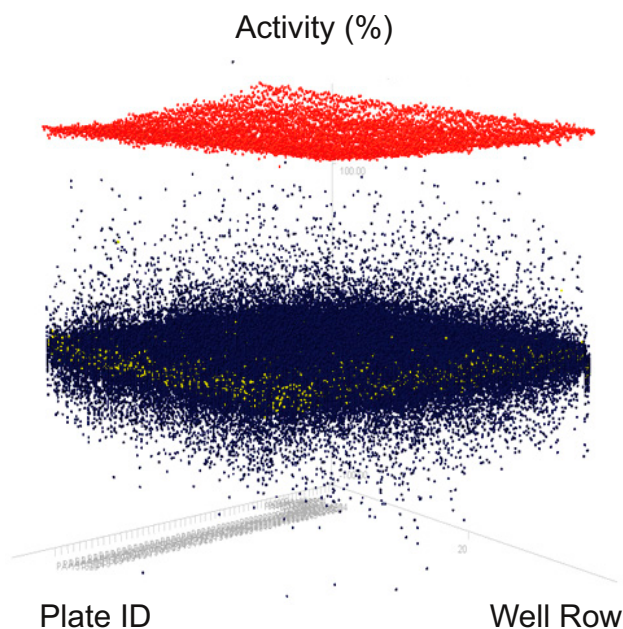
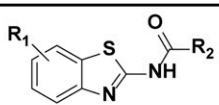
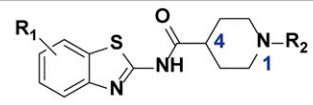


Fig. 1. HTS for GC-A potentiators. Three-dimensional scatter plot of test compounds at 10 μ M in the presence of 9 pM ANP (dark blue dots). As a positive (high) control (red dots), 5 nM ANP was used, and 9 pM ANP was used as negative (low) control (yellow dots). DMSO in all wells was <0.5%. $Z' = 0.87$.

solubility, and complete dose–response and potency criteria led to the prioritization of the 2-aminoacylbenzothiazole scaffold, represented by primary hit Compound 1 (Fig. 24). As illustrated in *SI Appendix, Fig. 1*, Compound 1 was specific in stimulating GC-A in the presence of an EC_{30} concentration of ANP and exhibited micromolar potency and efficacy (EC_{50} of 3.63 μ M and E_{max} of 80%) compared to saturating concentrations of ANP. Further, Compound 1 was devoid of activity in HEK293 GC-A cells tested in the absence of ANP and devoid of activity in HEK293 GC-B cells in the presence of CNP, thus supporting GC-A specificity and potentiation. Compound 1 had good compound solubility and mouse microsomal stability and was a promising starting point for synthesis of analogs and structure-activity relationship (SAR) studies in support of a focused hit to lead program.

Hit to Lead SAR Studies. Preliminary SAR of the 2-aminoacyl benzothiazole series is shown in Fig. 2. The resynthesized hit (Compound 1) retained the activity of the screening hit and confirmed the structural identity of the compound. Alkyl and cycloalkyl groups were preferred at R_2 position, and aryl groups led to complete loss of activity. Potency of analogs increased with size of the alkyl group (Fig. 24, Compounds 2, 3 vs. 1), and *N*-acylation of cycloalkyl derivatives in piperidine (6-membered) and pyrrolidine (5-membered) analogs led to significant improvements over hit Compound 1 (Fig. 24, Compounds 4 and 5). Next, we focused our SAR efforts on the substitution of *N*-acyl groups in the *N*-pivaloylpiperidine derivatives, and the results are listed in Fig. 2B. We found that *N*-acyl groups smaller than pivaloyl were tolerated (Fig. 2B, Compounds 6 and 7), and interestingly, *N*-alkyl groups such as isopropyl (Fig. 2B, Compound 8) had improved activity. The systematic screening of aromatic substitution at R_1 position was limited by lack of availability of commercial building blocks; however, changing 4,6-difluoro substitution in Compound 4 (Fig. 2A) to a 4,7-dichloro analog led to complete loss of activity (Fig. 2B, Compound 9). The 4-chlorobenzothiazole analog (Fig. 2B, Compound 10) retained all the activity of Compound 1,

 A 2-aminoacylbenzothiazole scaffold SAR				
Compound	R ₁	R ₂	EC ₅₀ (μM)	E _{max} (%)
1, hit	4,6-difluoro	-cyclohexyl	3.63	80
2	4,6-difluoro	-CH ₃	24.0	60
3	4,6-difluoro	-cyclobutyl	12.2	74
4	4,6-difluoro	-N-CO- <i>t</i> -Bu	2.18	83
5	4,6-difluoro	-N-CO- <i>t</i> -Bu	2.09	84

 B piperidine-4-carboxamide analogs				
Compound	R ₁	R ₂	EC ₅₀ (μM)	E _{max} (%)
6	4,6-difluoro	CO-cyclobutyl	1.72	79
7	4,6-difluoro	CO-Me	1.15	74
8	4,6-difluoro	<i>i</i> -Pr	0.84	80
9	4,7-dichloro	CO- <i>t</i> -Bu	>66	NA
10	4-Chloro	CO- <i>t</i> -Bu	2.00	51

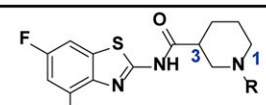
 C piperidine-3-carboxamide analogs			
Compound	R	EC ₅₀ (μM)	E _{max} (%)
11	CO- <i>t</i> -Bu	5.07	73
12	CO-cyclobutyl	1.81	77
13	CO-cyclopropyl	1.97	82
14	CO-Me	1.65	79
15	CO-phenyl	3.36	64
16	CO-benzyl	2.02	71
17	SO ₂ Me	1.75	77
18	CO-CH ₂ - <i>t</i> -Bu	3.57	74
19	CO ₂ - <i>t</i> -Bu	8.26	64
20	H	1.05	82
21	Me	1.23	81
22	benzyl	2.41	66
23 MCUF-651	CH ₂ CH ₂ N(Me) ₂	0.45	82

Fig. 2. SAR studies and hit to lead development of MCUF-651 (Compound 23). (A) SAR of 2-aminobenzothiazole scaffold, (B) SAR of piperidine-4-carboxamide analogs, and (C) SAR of piperidine-3-carboxamide analogs. The core scaffold is indicated for each table. Substituents for R, R₁, and R₂ are listed in the table sections along with the corresponding EC₅₀ and E_{max} values resulting from the synthetic change in the primary GC-A potentiation assay.

suggesting that 4,6-disubstitution may not be essential. Concurrent to the aforementioned efforts with piperidine-4-carboxamide analogs in Fig. 2B, piperidine-3-carboxamide analogs (Fig. 2C) were synthesized and tested in the HEK293 GC-A/cGMP assay. A 20-fold range in activity was observed with a trend consistent with the piperidine-4-carboxamide analog (Fig. 2C). R group could be an acyl or an alkyl group (Fig. 2C, Compounds 11 to 23). Small *N*-acetamide and methylsulfonamide analogs were most active among the *N*-acylated analogs (Fig. 2C, Compound 14 and 17). Extending the *t*-butyl group (in pivaloyl amide) to neopentyl group or the *t*-butyl carbamate with a -CH₂-linker or -O-linker, respectively (Fig. 2C, Compounds 11 vs. 18 and 19), led to significant erosion in activity. *N*-alkyl substitution led to active analogs (Fig. 2C, Compounds 20 to 23), including the unsubstituted piperidine analog (R = H, Fig. 2C, Compound 20). These results indicate a sterically demanding interaction with the target that potentially favors substituents with small three-dimensional size. Surprisingly, *N,N*-dimethylaminoethyl group with a longer alkyl spacer and a basic amine led to significant jump in potency (Fig. 2C, Compound 23), potentially due to likely favorable H-bonding interactions with the target. Compound 23 became our lead compound referred to as **MCUF-651** and represents an eightfold improvement in potency over hit Compound 1 (Fig. 24). The synthesis of MCUF-651 and analogs is depicted and described in *SI Appendix*, Fig. 2, and analytical data are shown in *SI Appendix*, Figs. 3–5.

Biological Profile of MCUF-651 In Vitro. From the aforementioned hit to lead efforts, we identified MCUF-651 as the lead

selective GC-A PAM, as it was able to potentiate ANP-mediated cGMP (Fig. 3A and B) and with a potency of EC₅₀ = 0.45 μM in HEK293 GC-A cells. MCUF-651 was devoid of cGMP generating activity in HEK293 GC-A cells in the absence of ANP as well as in HEK293 GC-B cells in absence and presence of CNP (Fig. 3A and *SI Appendix*, Fig. 6). The lack of agonist response of MCUF-651 alone further indicates that MCUF-651 is modulating ANP target engagement. Thus, MCUF-651 was specific for GC-A and stimulated cGMP generation in a dose-dependent fashion only in PAM mode. To highlight the mode of action as a PAM, we titrated ANP in the absence or presence of MCUF-651 (Fig. 3C). Increasing concentrations of MCUF-651 shifted the ANP-mediated cGMP dose-response curve to the left (or greater potencies), with no effect on maximal ANP concentration, indicating a PAM without agonist activity. The EC₅₀ value of ANP alone was 3.2 pM, and the EC₅₀ values of ANP in the presence of increasing concentrations of 0.1, 0.5, 1.0, 5.0, and 10 μM MCUF-651 decreased to 2.3, 1.6, 1.1, 0.7, and 0.6 pM, respectively, resulting in an overall 5-fold increase in affinity of ANP for GC-A when in the presence of 10 μM MCUF-651 compared to ANP alone. From the data in Fig. 3C, we determined the change in the percent cGMP response of the EC₃₀ concentration of the ANP (1.3 pM in the 384 well dose-response assay) curve in the absence of MCUF-651 (log EC₃₀ = 11.90) to the ANP curves in the presence of increasing concentrations of MCUF-651. The percent cGMP response change of the EC₃₀ concentration was plotted versus the corresponding concentration of MCUF-651

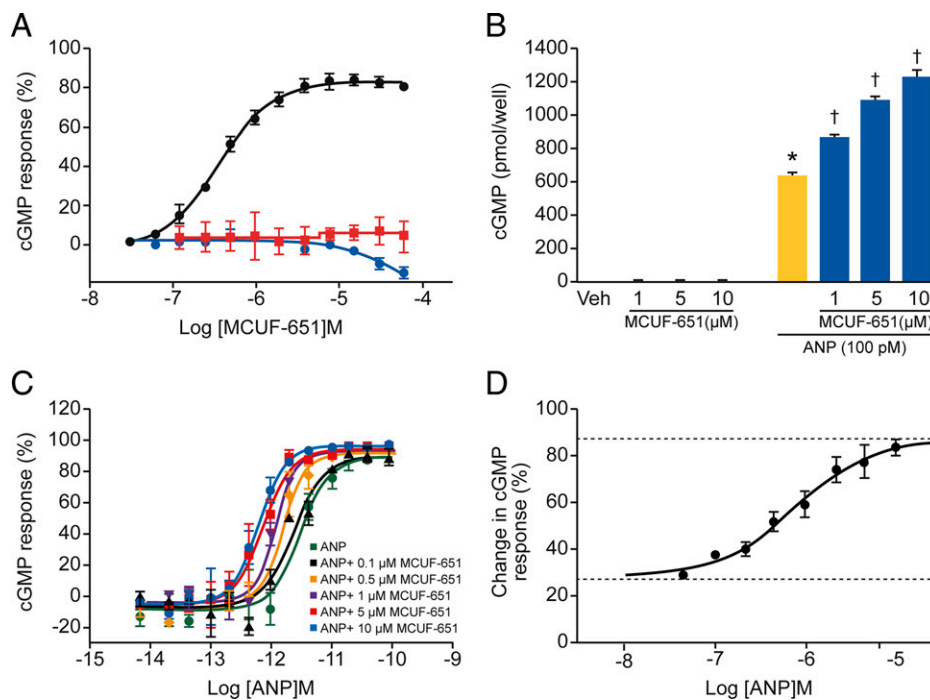


Fig. 3. Activation of MCUF-651 in HEK293 cells. (A) Percent cGMP response curves for cGMP response of MCUF-651 in HEK293 GC-A cells in the presence (black) and absence (red) of ANP (9 pM) and cGMP response of MCUF-651 in HEK293 GC-B cells in the presence (blue) of CNP (300 nM). (B) cGMP generation of vehicle, MCUF-651 alone, ANP alone (yellow bar), and ANP in the presence of MCUF-651 (blue bars) in HEK293 GC-A cells. Data are the average of two independent experiments and is expressed as mean \pm SEM. * P < 0.05 versus Veh; † P < 0.05 versus ANP alone. (C) Percent cGMP response curves in HEK293 GC-A cells in the presence of ANP titrated alone (green) and ANP titrated together with 0.1 (black), 0.5 (orange), 1 (purple), 5 (red), or 10 μ M (blue) MCUF-651. (D) Change in percent cGMP response for the EC₃₀ concentration of ANP (1.3 pM) in the presence of increasing concentrations of MCUF-651. Data in A, C, and D are the average of three independent experiments and are expressed as mean \pm SD.

(Fig. 3D). This graph is referred to as the EC₃₀ sensitivity assay. Nonlinear regression analysis of this data resulted in $pEC_{50} = 6.1 \pm 0.2$ ($EC_{50} = 0.80 \mu M$), which provides a quantitative assessment of intrinsic PAM affinity.

Surface plasmon resonance (SPR) analysis was conducted for binding of MCUF-651 or ANP alone and MCUF-651 in the presence of increasing concentrations of ANP to the extracellular domain of human GC-A. We confirmed the binding of MCUF-651 alone to human GC-A to have K_D equal to 397 nM (Table 1). Strong binding of ANP at increasing concentrations to human GC-A was validated with a K_D of 0.72 nM (Table 1 and Fig. 4A). Importantly, the K_D was shifted lower to 0.06 nM in the presence of MCUF-651 (10 μ M) and increasing concentrations of ANP (Table 1 and Fig. 4B). Additionally, SPR studies showed MCUF-651 also enhanced the binding of BNP to human GC-A (SI Appendix, Table 1) and had very low affinity to human GC-B and did not alter the binding affinity of CNP to GC-B (SI Appendix, Table 2). Together, these findings further corroborate that MCUF-651 is a selective GC-A PAM.

Table 1. SPR binding kinetics for MCUF-651 and ANP to human GC-A receptor

	k_a ($M^{-1} \cdot s^{-1}$)	k_d (s^{-1})	K_D (nM)
MCUF-651	5.8×10^4	2.3×10^{-2}	397
ANP	2.5×10^7	1.8×10^{-2}	0.72
MCUF-651 + ANP	3.3×10^8	1.9×10^{-2}	0.06

MCUF-651 alone binds to GC-A. MCUF-651 (10 μ M) further enhanced the binding affinity of ANP to GC-A by increasing the association rate of ANP to GC-A, thus reducing the equilibrium dissociation rate. k_a , association rate; k_d , dissociation rate; K_D , equilibrium dissociation rate.

Next, to support the therapeutic potential of MCUF-651 on biological actions via GC-A, we determined cGMP generation in response to increasing doses of MCUF-651 in the presence of a low dose of ANP (100 pM) in HRPTCs, HAs, and HCMs as well as the antihypertrophic actions in HCMs. Illustrated in Fig. 5A–C and SI Appendix, Fig. 7 are the cGMP levels in HRPTCs, human visceral adipocytes (HVAs), HCMs, and human subcutaneous adipocytes (HSAs), respectively, to increasing concentrations of MCUF-651 in the presence of ANP. Notably, the potentiation of cGMP of MCUF-651 in HCMs, in particular, led to a favorable functional response in our state-of-the-art live cell imaging platform. As illustrated in Fig. 5D, exposure to TGF β -1 resulted in a significant increase in HCM cell surface area, and treatment with a low dose of ANP did not inhibit the TGF β -1 induced increase in HCM cell surface area. However, treatment with a low dose of ANP, together with MCUF-651, resulted in a significant inhibition of HCM hypertrophy induced by TGF β -1. These data support the concept that positive allosteric modulation of GC-A with MCUF-651 has the potential to mediate protection in human cells related to CV disease as well as its associated risk factors, such as renal dysfunction and obesity.

In Vivo PK and Bioavailability in Mice. In vivo PK studies in mice showed MCUF-651 is bioavailable at 24 h when given orally or IV (Fig. 6). MCUF-651 had good clearance and exposure (SI Appendix, Fig. 8; clearance: 20.3 mL/min/kg, steady-state volume of distribution: 16.8 L/kg, half-life: 10.9 h after 5 mg/kg IV dose; peak plasma concentration: 605 ng/mL, half-life: 9.1 h, area under the curve: 7,095 ng \cdot h/mL after 10 mg/kg oral dose) and met our internal metrics as a lead compound.

Ex Vivo MCUF-651 Potency in Human Plasma. To further define the therapeutic potential of MCUF-651, we developed an ex vivo

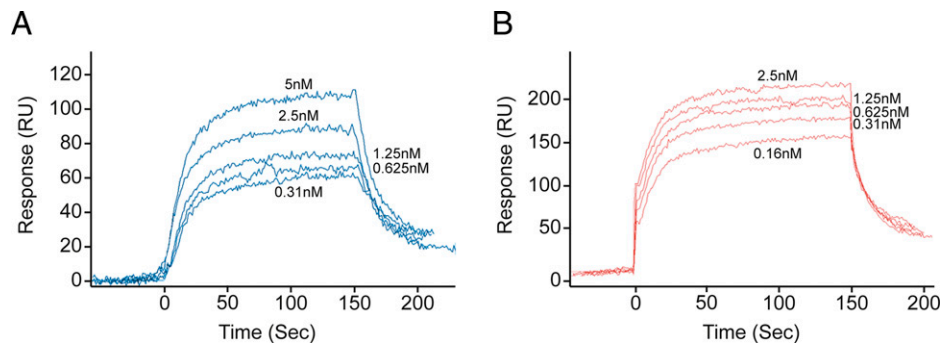


Fig. 4. SPR binding GC-A binding curves for ANP and MCUF-651. (A) Representative SPR sensorgram for the binding of ANP alone (blue) to the extracellular domain of human GC-A. (B) Representative SPR sensorgram for binding of increasing concentrations of ANP in the presence of MCUF-651 (10 μ M; red) to the extracellular domain of human GC-A.

potency assay in which we utilized human plasma from normal subjects and patients with hypertension and HF ($n = 6$ per group), who have various levels of circulating ANP and BNP, the endogenous ligands of GC-A. Table 2 reports subject characteristics and their respective plasma ANP and BNP levels. As illustrated in Fig. 7, MCUF-651 potentiated the generation of cGMP levels in HEK293 GC-A cells in all three cohorts. Importantly, MCUF-651 demonstrated greatest cGMP potency in HF plasma in which ANP and BNP circulating levels were the highest. Thus, our ex vivo findings provide validation that MCUF-651 possesses GC-A enhancing action in human plasma and operates in a PAM mode with increasing cGMP generation in association with increasing concentrations of endogenous ANP and BNP.

Discussion

Almost four decades of research have supported the pivotal role of GC-A/cGMP signaling in regulating BP and intravascular volume homeostasis via activation by its endogenous cardiac-derived ligands, ANP and BNP (4, 6, 16). Beyond BP regulation, the ANP/BNP/GC-A/cGMP pathway also possesses key protective biological actions that include the suppression of adverse cardiorenal and CV remodeling, inhibition of the RAAS, promotion of adipocyte lipolysis, lipid oxidation, and the browning of white adipocytes (4–6). Accordingly, the GC-A represents an attractive molecular target for therapeutic intervention. Indeed, synthetic or recombinant peptide forms of ANP (carperitide) and BNP (nesiritide) have been approved

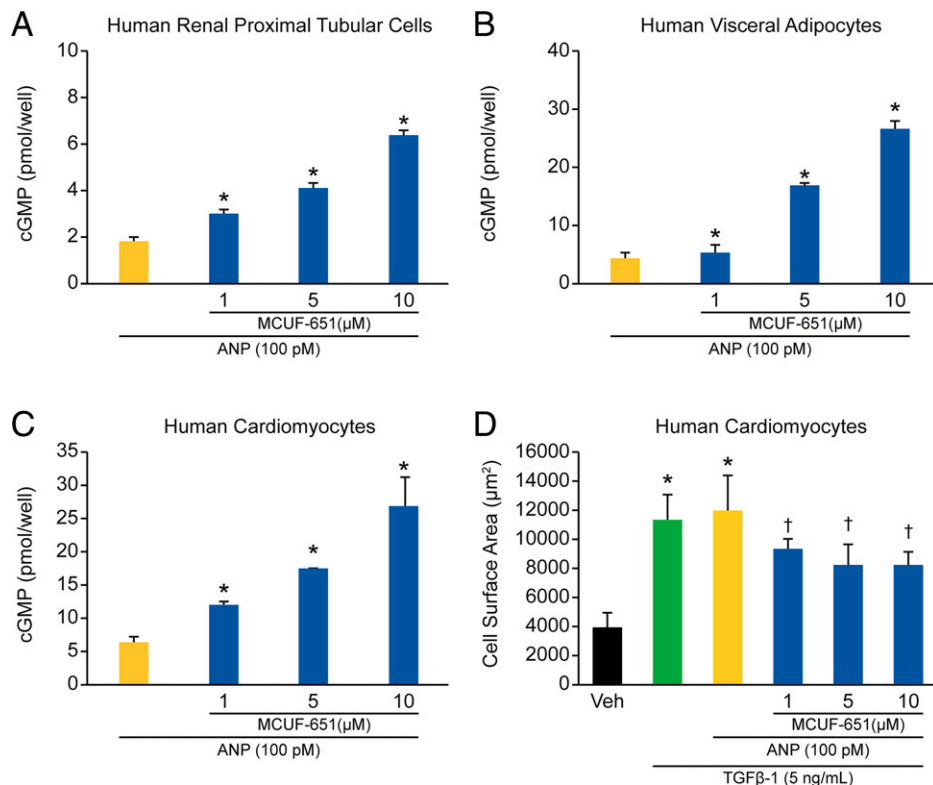


Fig. 5. Effect of MCUF-651 on human primary cells. (A) Generation of cGMP in HRPTCs, (B) HVAs, and (C) HCM stimulated by ANP alone (yellow bar) or together in the presence of MCUF-651 (blue bars). Data are the average of two independent experiments and are expressed as mean \pm SEM. * $P < 0.05$ versus ANP alone. (D) Inhibition of TGF β -1 induced HCM hypertrophy (reduction in cell surface area) by ANP in the presence of MCUF-651 (blue bars). Data are the average of two independent experiments and are expressed as mean \pm SEM. * $P < 0.05$ versus Veh (black bar). † $P < 0.05$ versus TGF β -1 alone (green bar).

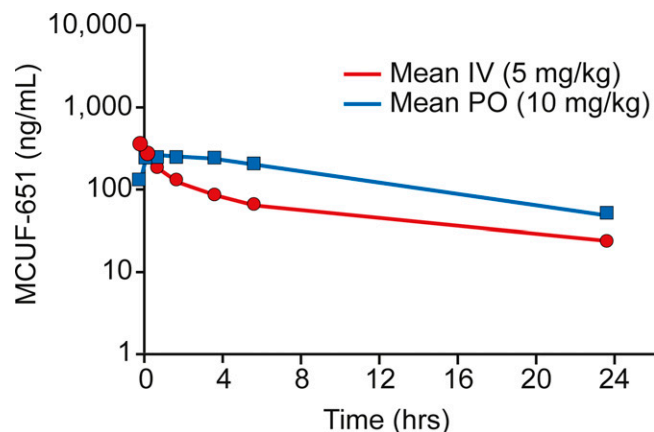


Fig. 6. In vivo bioavailability of MCUF-651. Plasma concentrations of MCUF-651, administered orally (blue) or IV (red), in mice ($n = 3/\text{route}$) over 24 h.

for the IV treatment of acute HF in Japan and the United States, respectively (8, 9). To optimize receptor activation, delivery, and circulating bioavailability, designer NPs have been engineered and include the novel ANP analog, MANP, which is in clinical trials for resistant hypertension (17). Thus, the discovery and development of GC-A targeted small molecules, which to date do not exist, to potentiate GC-A signaling of its endogenous ligands ANP and BNP and be orally bioavailable would represent a major breakthrough in CV therapeutics.

Multiple investigations have established the pleiotropic actions of GC-A in myocardial, renal, and metabolic regulation, as the GC-A receptor is highly expressed in the heart, kidney, and adipose tissue (4). Many studies have validated the antihypertrophic and antiapoptotic actions via the GC-A/cGMP pathway in cardiomyocytes complemented by natriuretic actions in the kidney and favorable metabolic actions in adipocytes (18–23). We therefore investigated if MCUF-651 would operate as a PAM in human primary myocardial and renal cells as well as in HAs. In a dose-dependent manner, MCUF-651 potentiated ANP-mediated cGMP generation in HCMs, HRPTCs, HVAs, and HSAs. This finding is of particular interest as it demonstrates the direct enhancement of GC-A/cGMP signaling beyond the use of augmenting peptide ligands. Moreover, as key biological properties of the GC-A include the suppression of cardiac hypertrophy and renal tubular cell apoptosis, natriuresis, adipocyte lipolysis, and lipid oxidation, the potentiation of cGMP with MCUF-651 in these human primary cells provides evidence of the protective capabilities of this small molecule in CVD and in diseases of renal dysfunction as well as in obesity. Indeed, the antihypertrophic actions in HCMs provide functional evidence that the potentiation of cGMP via GC-A signaling with MCUF-651 has biological significance. Nonetheless, additional studies are warranted to further evaluate the protective actions of MCUF-651 both in vitro and in vivo.

Table 2. Human subject and patient characteristics

	Normal subjects ($n = 6$)	Hypertensive patients ($n = 6$)	HF patients ($n = 6$)
Age, years	59 ± 8	69 ± 9	65 ± 10
Sex, female (%)	75%	50%	75%
BMI, kg/m ²	28 ± 3	25 ± 1	29 ± 5
eGFR, mL/min/1.73 m ²	75 ± 15	70 ± 8	50 ± 25
ANP, pg/mL	26 ± 12	13 ± 8	350 ± 140
BNP, pg/mL	27 ± 14	59 ± 37	1,226 ± 711

BMI, body mass index; eGFR, estimated glomerular filtration rate. Values are presented as mean ± SD, n (%).

Our discovery and findings highlight a paradigm that is built on the concept of allosterism, which is a process by which a molecule binds to one site, often distal to the functional site, allowing for regulation of activity (24). Our SPR binding studies demonstrate that MCUF-651 alone binds to GC-A with >500-fold less affinity than ANP. Notably, MCUF-651, in the presence of ANP, enhances the binding affinity of ANP to GC-A by reducing the equilibrium dissociation rate. Based on the elegant crystal structural data of GC-A (25, 26), we speculate that MCUF-651 binds to an allosteric site in the extracellular domain of GC-A, which induces a favorable conformational change that, in turn, enhances the ability of ANP to engage the binding pocket more effectively. This is supported by our SPR data that show a faster association rate of ANP in the presence of MCUF-651, resulting in a greater engagement of ANP with the binding pocket. Because the disassociation rate does not change, the residence time of ANP at the GC-A target is not affected in the presence of MCUF-651. Thus, it is the faster association rate and better target engagement, which lowers the energy of activation, that is driving the increase in potency of ANP in the presence of MCUF-651. This increase of potency for ANP due to better target engagement is translated into greater cGMP production via GC-A as further supported by data in Fig. 3C showing that ANP induces the same magnitude of cGMP production at fivefold less concentration in the presence of MCUF-651 than ANP does alone. This paradigm in regulating GC-A/cGMP signaling, with a PAM, lays the foundation for a direction in GC-A therapeutics.

The therapeutic delivery strategy for enhancing GC-A in CVD, especially HF, has been predominantly IV administration of recombinant ANP or BNP for short periods of time. We reported efficacy of chronic subcutaneous injection of BNP for 8 wk in patients with stable HF (27). Indeed, chronic SQ BNP compared to placebo reduced left ventricular mass as determined by NMR and reduced LV systolic volume. Further, the activation of cGMP was sustained throughout the 8-wk treatment period. To date, there exists no oral delivery platform for NPs in humans.

Based upon the chemical characteristics of MCUF-651, we determined the bioavailability of oral delivery in conscious mice. This goal was driven by the high impact of advancing our small molecule GC-A PAM to an orally deliverable drug, which would have potentially game-changing implications for chronically enhancing the GC-A/cGMP pathway for CVD and beyond. Herein, we observed that MCUF-651 is orally bioavailable up to 24 h after administration, thus strengthening the potential clinical impact of this small molecule GC-A targeted drug.

To further establish the clinical potential of MCUF-651 in humans, we developed a highly innovative MCUF-651 potency assay to mimic the administration of our GC-A PAM to normal subjects and patients with hypertension and HF in an ex vivo setting. Here, we administered MCUF-651 to plasma from normal subjects, hypertensive patients, and patients with HF and applied to HEK293 cells overexpressing GC-A to determine its ability to potentiate cGMP generation. Here, we observed a

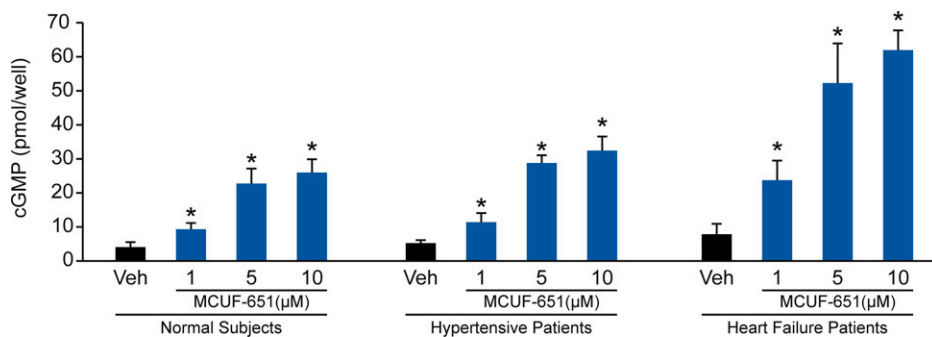


Fig. 7. Effect of MCUF-651 in human plasma. cGMP generation of MCUF-651 (blue bars) in HEK293 GC-A cells when incubated with human plasma from normal subjects, hypertensive patients, and HF patients ($n = 6/\text{group}$) of which endogenous ANP and BNP levels are present. Data are the average of two independent experiments and are expressed as mean \pm SEM. * $P < 0.05$ versus Veh (black bar) within each subject group.

dose-dependent increase in cGMP generation in our potency assay in all three cohorts, with HF patients, which had the highest levels of endogenous ANP and BNP, exhibiting the greatest response in cGMP generation. This *ex vivo* finding provides a signal of the potential therapeutic efficacy that may be seen in human clinical trials when testing a small molecule GC-A PAM. Indeed, MCUF-651 may offer another yet unique strategy to optimize the GC-A/cGMP pathway beyond exogenous native or designer NPs and NEP inhibition with S/V. As PAMs are self-titrating, it is tempting to speculate that MCUF-651 can be of therapeutic benefit in either low or high NP and/or GC-A states. Furthermore, as a small molecule, MCUF-651 can be given orally, as seen here, which has been a major challenge for NP therapeutics to date.

In summary, we report the discovery and development of an oral small molecule GC-A PAM that is active in human myocardial, renal, and adipose cells and exhibits therapeutic potential by potentiating cGMP using plasma samples from normal subjects and patients with hypertension and HF, *ex vivo*. These studies provide a proof-of-concept that the GC-A/cGMP signaling pathway can be uniquely enhanced with a small molecule PAM. Such a discovery supports its further development as a game changing therapeutic strategy to reduce the rising global burden of death related to its number one cause, CVD, as well as its major risk factors of hypertension, obesity, and renal dysfunction.

Materials and Methods

Peptides and Compounds. Human ANP and CNP (Phoenix Pharmaceutical) were dissolved in water at 500 mM stock and aliquoted and stored at -20°C . Compound 1 (CAS# 868368-67-6) was purchased from LifeChem (F1813-1161). Compounds (Entry) 2 to 23 were synthesized and purified at the Chemical Genomics Center at Sanford Burnham Prebys Medical Discovery Institute (Orlando, FL). All other chemicals and reagents were from Sigma-Aldrich. The identity and purity of MCUF-651 was confirmed using ^1H nuclear magnetic resonance (NMR), liquid chromatography-mass spectrometry (LC-MS) trace, and mass spectrometry (MS) spectrum (SI Appendix, Figs. 3–5).

Cell Culture for HTS. HEK293 cells overexpressing human GC-A and GC-B (Cardiorenal Research Laboratory, Mayo Clinic) and the parental cell line (American Type Culture Collection CRL-1573) devoid of either GC receptors were cultured in growth media consisting of Dulbecco's modified Eagle medium (DMEM) (Corning; no. 10013CM) containing 1% L-glutamine and sodium pyruvate and supplemented with 10% fetal bovine serum (HyClone; SH30396.03), 500 $\mu\text{g}/\text{mL}$ G418 (Thermo Fisher; no. 10131035) (28, 29). Cell cultures were maintained in cell culture incubator at 37°C in 5% CO_2 and were routinely subcultured twice weekly by trypsin-ethylenediaminetetraacetic acid (EDTA) treatment (0.05% trypsin-EDTA). The cells in an exponential growth phase were harvested, counted, and cryopreserved at high density 6 to 15 million cells/mL for suspension assays. On the day of the assay, cells were thawed, counted, and resuspended in assay media (OptimMem containing

2% heat-activated fetal bovine serum and 1% L-glutamine) and used as described as follows in HTS cGMP production.

HTS cGMP Production. In our effort to identify GC-A PAMs from the NIH MLSMR, we developed a primary cell-based screening assay to monitor the production of cGMP, the second messenger generated by GC-A activation, by homogenous time-resolved fluorescence (HTRF) competition assay using labeled-cGMP in HEK293 cells overexpressing the human GC-A receptor. Compound EC_{50} values were determined in the primary cell-based screening assay, in the presence or absence of ANP, to determine mode of action as positive modulators and tested for selectivity in the same assay platform but in HEK293 cells overexpressing human GC-B, for which CNP is the endogenous ligand and not ANP. For HTS, GC-A suspension cells were plated in 1,536 well and stimulated in the presence of 10 μM compound concentration and a sub-maximal concentration of ANP. The quantity of cGMP was detected by HTRF and normalized to maximal amount produced by ANP.

Specifically, 20 nL of 10 mM test compounds in dimethyl sulfoxide (DMSO) from the NIH MLSMR (370,620 test compounds) were added to columns 5 to 48 of 1,536 well white high base screening plates (Corning) cells using 550 ECHO acoustic dispenser (Labcyte). ANP was prepared as working stock aliquots at 5 μM in phosphate-buffered solution (PBS) with 0.1% bovine serum albumin (BSA). An approximate EC_{30} concentration of ANP (9 pM) in assay buffer (Hanks' Balanced Salt Solution [HBSS] containing 5 mM Hepes and 0.05% BSA) was added to columns 3 to 48 at a volume of 1 μL . Assay buffer only was added to column 1, and assay buffer containing a saturating concentration of ANP (5 nM) was added to column 2. HEK293 cells overexpressing human GC-A in assay media were stirred continuously for 2 h at room temperature (RT) at a density of 6×10^5 cells/mL and 2 μL were plated in screening plates (1,200 cells/well) using a Bioraptr 2. Plates were spun at 1,000 rpm for 1 min and incubated for 30 min at RT. The 1.5 μL d2-labeled cGMP followed by 1.5 μL Eu3+ cryptate-labeled anti-cGMP cGMP detection kit (CisBio; #62GM2PEC) prepared according to manufacturer's protocol were added to all wells using a Bioraptr 2, and TR-FRET signal was detected on an EnVision detector (PerkinElmer). Wells treated with 0.3% DMSO served only as blank controls (column 1), wells treated with 0.3% DMSO and 5 nM ANP (columns 2) served as positive controls, and wells treated with 0.3% DMSO and 9 pM ANP (columns 3 to 4) served as negative controls. DMSO did not exceed 0.3% in all wells.

EC_{50} cGMP Determination. Test compounds at 10 mM DMSO stock concentration were added to 1,536 or 384 well assay plates using Echo dispensing starting at 80 μM concentration and diluted 2-fold for 10-point concentration-response curves. Wells were backfilled with DMSO such that the final concentration of DMSO in all wells was maintained at 0.3% DMSO. Agonist response (absence of ANP) and positive allosteric modulation (presence of EC_{30} concentration of ANP at 1.3 pM in the 384 well dose-response assay (9 pM in the HTS 1536 well assay) of GC-A-mediated activation of cGMP production was measured in human GC-A-overexpressing HEK293 cells using cGMP CisBio detection kit (as described previously). For selectivity assays, compounds were tested in human GC-B overexpressing HEK293 cells in the presence of an EC_{30} concentration of CNP (3 nM), the endogenous ligand for GC-B. For counter screen assays, compounds were tested using the same protocol but in parental HEK293 cells and in the presence of 9 pM ANP. A 100% response was determined from wells in the absence of compound and presence of saturating concentration of ANP (5 nM) or CNP (300 nM), and 0% response was determined from wells containing an EC_{30} concentration of ANP or CNP determined

on the day of the assay. Compounds were further tested for the absence of PDE5 inhibition using the PDE5A1 assay kit (BPS Bioscience) with 8 pg/mL PDE5A enzyme and Sildenafil as a control according to manufacturer's protocol.

cGMP Levels in HEK293 Cells Overexpressing Human GC-A and GC-B. HEK293 GC-A or GC-B cells were seeded in 48-well plates (1×10^5 cell per well) and cultured overnight to reach 80 to 90% confluency. The treatment buffer that consists of HBSS, 0.1% BSA, 2 mM Hepes, and 0.5 mM 3-isobutyl-1-methylxanthine (a nonspecific phosphodiesterase inhibitor) was used in all experiments. MCUF-651 was dissolved in DMSO; ANP and CNP were dissolved in PBS. On the experimental day, growth media was replaced with treatment buffer and HEK293 GC-A and GC-B cells were pretreated with MCUF-651 at doses of 1, 5, or 10 μ M (reaching a final concentration of 0.1% DMSO) for 5 min at 37 °C. Afterward, HEK293 GC-A cells were treated with ANP (100 pM) and HEK293 GC-B cells treated with CNP (100 pM) for additional 10 min at 37 °C. HEK293 GC-A and GC-B cells were also treated with vehicle (0.1% DMSO) which served as a negative control. Then, all cells were washed with PBS once and lysed with 0.1 M HCl. Intracellular cGMP was measured in the lysate using a commercial cGMP ELISA Kit (Enzo Life Sciences) as instructed by the manufacturer.

cGMP Levels in Human Primary Cells with MCUF-651. Human primary cardiomyocytes (HCMs; Catalog No. 6200, Lot No. 6288, PromoCell) and human primary renal proximal tubular cells (Catalog No. 4100, Lot No. 5111, ScienCell) were maintained and subcultured according to the manufacturer's protocols. Human visceral preadipocytes (Catalog No. 7210, Lot No. 0731, ScienCell) and subcutaneous preadipocytes (Catalog No. 7220, Lot No. 0928, ScienCell) were differentiated into mature HVAs and HSAs according to the manufacturers' protocol. Passages 4 to 8 were used in the study. Treatment buffer, MCUF-651, ANP, and vehicle were prepared as described previously. Briefly, 5×10^5 cells/well were grown in 6-well plates until 80 to 90% confluency and were then pretreated with vehicle or MCUF-651 at doses of 1, 5, or 10 μ M for 5 min at 37 °C, then cells were treated with ANP (100 pM) for an additional 10 min at 37 °C. Afterward, all cells were washed with PBS once and lysed with 0.1 M HCl at RT, and intracellular cGMP levels were measured in the lysate using a commercial cGMP ELISA kit (Enzo Life Sciences) with the acetylation method as instructed by the manufacturer.

HCM Hypertrophy Assay. HCM (same as previously mentioned) hypertrophy was evaluated using the automated live-cell, real-time imaging IncuCyte S3 system (Essen BioScience). MCUF-651 and ANP were prepared as described previously, vehicle was prepared as 0.1% DMSO, and TGF- β 1 (R&D Systems) was prepared in 4 mM HCl and 0.1% BSA in PBS. HCMs were plated in 96-well plates (1,000 cells/well) and incubated in growth media at 37 °C overnight and then were subjected to differentiation by serum starvation for 24 h. Afterward, TGF- β 1 (5 ng/mL) was added to the media for 48 h to induce HCM hypertrophy (increase in cell surface area). Then, cells were treated with ANP (100 pM) with vehicle or ANP (100 pM) with MCUF-651 at doses of 1, 5, or 10 μ M for another 48 h. HCM treated with vehicle alone served as a negative control, while TGF- β 1 together with vehicle served as a positive control. Images were taken continuously during the study period as instructed by the manufacturer, and the analysis for cell surface area (micrometers squared) was performed using the ImageJ software.

GC-A and GC-B Binding Studies. SPR measurements were performed at 25 °C on a BI-4500 SPR instrument (Biosensing Instrument Inc.) (30). As per the instructions by the Biosensing instrument manual, 400 mM nickel sulfate in deionized water was linked to the Ni-NTA sensor chip (Biosensing Instrument, Inc.). Then, 40 μ g/mL of extracellular domain human GC-A or GC-B recombinant protein (MyBioSource, Inc.), containing 12 histidine residues on the C terminus, was then immobilized to the nickel sulfate on the Ni-NTA sensor chip. Afterward, the chip was washed with buffer (150 mM NaCl, 50 μ M EDTA pH 7.4, 0.1% DMSO), then 150 μ L of sequentially diluted MCUF-651 (0.625, 1.25, 2.5, 5, 10 μ M for GC-A receptor or 1.25, 2.5, 5, 10, 20 μ M for GC-B receptor) alone was injected at the rate of 60 μ L/min and allowed to dissociate for 60 s. For GC-A binding studies with ANP or BNP, 150 μ L of sequentially diluted ANP

or BNP (0.31, 0.625, 1.25, 2.5, and 5 nM) alone, or ANP (0.16, 0.31, 0.625, 1.25, and 2.5 nM) or BNP (0.31, 0.625, 1.25, 2.5 and 5 nM) together with MCUF-651 (10 μ M) were injected at the rate of 60 μ L/min and allowed to dissociate for 200 s. For GC-B binding studies with CNP, 150 μ L of sequentially diluted CNP (0.31, 0.625, 1.25, 2.5 and 5 nM) alone or CNP (0.31, 0.625, 1.25, 2.5 and 5 nM) together with MCUF-651 (10 μ M) were injected at the rate of 60 μ L/min and allowed to dissociate for 200 s. Data were collected as sensorgrams. Binding kinetics were derived from sensorgrams using BI-Data Analysis Program (Biosensing Instrument). Affinity analysis of GC-A with ANP, BNP, and/or MCUF-651 and GC-B with CNP and/or MCUF-651 interactions were performed using a 1:1 Langmuir binding model. Two series were performed for all studies.

Drug Metabolism and PK Studies. Mice were manipulated and housed according to the protocols approved by the Shanghai Medical Experimental Animal Care Commission. Drug metabolism and PK studies were performed at WuXi AppTec Co., Ltd. The test article was accurately weighed and mixed with DMSO:Tween80:water (1:1:8) and sonicated. The formulation was prepared fresh daily, and animals (three in each group, male C57BL/6, 7 to 9 wk) were dosed 2 h after the formulation was prepared. Aliquots of each formulation were dose validated by liquid chromatography with tandem mass spectrometry (LC/MS/MS). Oral (PO; per os) dosing was administered via oral gavage. The dose volume was determined by the animals' body weight collected on the morning of the dosing day. Serial bleeding (about 30 μ L blood per time point) was collected from submandibular or saphenous vein. All blood sample were transferred to microcentrifuge tube containing 2 μ L of K2EDTA (0.5 M) as anticoagulant and placed on ice until processed for plasma. Blood samples were processed for plasma by centrifugation at $3,000 \times g$, quickly frozen, and stored at -70 °C until quantification by LC/MS analysis.

Ex Vivo Human Therapeutic Potency Assay. Stored human plasma samples from normal subjects and patients with hypertension and HF were utilized. The details of the recruitment of these participants are previously reported (31, 32). All participants gave written informed consent, and the Institutional Review Board at Mayo Clinic approved this study. From all cohorts, plasma ANP was determined by a Mayo-developed ANP radioimmunoassay, while plasma BNP was measured using a two-site immunoenzymatic sandwich assay (Biosite Inc.) (7, 31, 33). HEK293 overexpressing human GC-A were cultured and grown as described previously. Cells were grown in 48-well plates to 80 to 90% confluence. On the day of the experiment, cells were pretreated with MCUF-651 at doses of 1, 5, or 10 μ M and without (vehicle) in 250 μ L treatment buffer (as described previously) for 5 min at 37 °C. Then, 25 μ L human plasma was added and incubated for an additional 10 min. Afterward, cells were washed with PBS once and lysed with 0.1 M HCl, and intracellular cGMP levels were measured in the lysate using a commercial cGMP ELISA Kit (Enzo Life Sciences) as instructed by the manufacturer.

Curve Fit and Statistical Analysis. All concentration-response curves were analyzed to determine EC_{50} and E_{max} using the following equation: $E_{max} = 100/[1 + 10^{(LogEC_{50}-X) \times \text{Hill slope}}]$, where X is the log of concentration of compound tested and the Hill slope is set equal to 1. All experiments were repeated at least three times. Data are expressed as mean \pm SEM or SD as indicated. Unpaired t test was performed for comparison between groups in HEK293 GC-A and GC-B cell, human primary cell, and therapeutic potency assay studies. Nonlinear regression curve fit and statistical analyses were performed using Prism 7 (GraphPad Software, Inc.).

Data Availability. All study data are included in the article and/or *SI Appendix*. Consistent with the goals of NIH funding, the primary assay data and protocols from HTS are available in PubChem under the following Assay ID (AID): 1671463.

ACKNOWLEDGMENTS. This work was funded by grants from the NIH (R01 DK103850 and R01 HL136340 to J.C.B.; R01 HL132854 to S.J.S.; and R01 AG056315 to S.J.S., S.M., and J.C.B.), Department of Cardiovascular Medicine, Mayo Clinic, and Mayo Foundation. We thank Paul Kung and Thomas D. Y. Chung for assistance in uploading screening and bioassay data into PubChem.

1. S. Sidney *et al.*, Recent trends in cardiovascular mortality in the United States and public health goals. *JAMA Cardiol.* **1**, 594–599 (2016).
2. G. A. Roth *et al.*; GBD-NHLBI-JACC Global Burden of Cardiovascular Diseases Writing Group, Global burden of cardiovascular diseases and risk factors, 1990–2019: Update from the GBD 2019 Study. *J. Am. Coll. Cardiol.* **76**, 2982–3021 (2020).
3. S. A. Waldman, R. M. Rapoport, F. Murad, Atrial natriuretic factor selectively activates particulate guanylate cyclase and elevates cyclic GMP in rat tissues. *J. Biol. Chem.* **259**, 14332–14334 (1984).

4. M. Kuhn, Molecular physiology of membrane guanylyl cyclase receptors. *Physiol. Rev.* **96**, 751–804 (2016).
5. J. P. Goetze *et al.*, Cardiac natriuretic peptides. *Nat. Rev. Cardiol.* **17**, 698–717 (2020).
6. K. N. Pandey, Molecular and genetic aspects of guanylyl cyclase natriuretic peptide receptor-A in regulation of blood pressure and renal function. *Physiol. Genomics* **50**, 913–928 (2018).
7. S. P. Murphy *et al.*, Atrial natriuretic peptide and treatment with sacubitril/valsartan in heart failure with reduced ejection fraction. *JACC Heart Fail.* **9**, 127–136 (2021).

8. Publication Committee for the VMAC Investigators (Vasodilatation in the Management of Acute CHF), Intravenous nesiritide vs nitroglycerin for treatment of decompensated congestive heart failure: A randomized controlled trial. *JAMA* **287**, 1531–1540 (2002).
9. Y. Saito, Roles of atrial natriuretic peptide and its therapeutic use. *J. Cardiol.* **56**, 262–270 (2010).
10. L. R. Potter, Natriuretic peptide metabolism, clearance and degradation. *FEBS J.* **278**, 1808–1817 (2011).
11. D. M. Dickey, A. R. Yoder, L. R. Potter, A familial mutation renders atrial natriuretic Peptide resistant to proteolytic degradation. *J. Biol. Chem.* **284**, 19196–19202 (2009).
12. P. M. McKie *et al.*, A human atrial natriuretic peptide gene mutation reveals a novel peptide with enhanced blood pressure-lowering, renal-enhancing, and aldosterone-suppressing actions. *J. Am. Coll. Cardiol.* **54**, 1024–1032 (2009).
13. P. R. Gentry, P. M. Sexton, A. Christopoulos, Novel allosteric modulators of G protein-coupled receptors. *J. Biol. Chem.* **290**, 19478–19488 (2015).
14. B. Roy, E. J. Halvey, J. Garthwaite, An enzyme-linked receptor mechanism for nitric oxide-activated guanylyl cyclase. *J. Biol. Chem.* **283**, 18841–18851 (2008).
15. J. B. Baell, G. A. Holloway, New substructure filters for removal of pan assay interference compounds (PAINS) from screening libraries and for their exclusion in bioassays. *J. Med. Chem.* **53**, 2719–2740 (2010).
16. K. D. Bloch, J. G. Seidman, J. D. Naftilan, J. T. Fallon, C. E. Seidman, Neonatal atria and ventricles secrete atrial natriuretic factor via tissue-specific secretory pathways. *Cell* **47**, 695–702 (1986).
17. L. M. G. Meems *et al.*, Design, synthesis, and actions of an innovative bispecific designer peptide. *Hypertension* **73**, 900–909 (2019).
18. M. Kuhn *et al.*, Progressive cardiac hypertrophy and dysfunction in atrial natriuretic peptide receptor (GC-A) deficient mice. *Heart* **87**, 368–374 (2002).
19. T. Kato *et al.*, Atrial natriuretic peptide promotes cardiomyocyte survival by cGMP-dependent nuclear accumulation of zyxin and Akt. *J. Clin. Invest.* **115**, 2716–2730 (2005).
20. S. K. Dubois, I. Kishimoto, T. O. Lillis, D. L. Garbers, A genetic model defines the importance of the atrial natriuretic peptide receptor (guanylyl cyclase-A) in the regulation of kidney function. *Proc. Natl. Acad. Sci. U.S.A.* **97**, 4369–4373 (2000).
21. M. Bordicchia *et al.*, Cardiac natriuretic peptides act via p38 MAPK to induce the brown fat thermogenic program in mouse and human adipocytes. *J. Clin. Invest.* **122**, 1022–1036 (2012).
22. P. M. Oliver *et al.*, Hypertension, cardiac hypertrophy, and sudden death in mice lacking natriuretic peptide receptor A. *Proc. Natl. Acad. Sci. U.S.A.* **94**, 14730–14735 (1997).
23. R. T. Lee *et al.*, Atrial natriuretic factor gene expression in ventricles of rats with spontaneous biventricular hypertrophy. *J. Clin. Invest.* **81**, 431–434 (1988).
24. H. N. Motlagh, J. O. Wrabl, J. Li, V. J. Hilser, The ensemble nature of allostery. *Nature* **508**, 331–339 (2014).
25. H. Ogawa, Y. Qiu, C. M. Ogata, K. S. Misono, Crystal structure of hormone-bound atrial natriuretic peptide receptor extracellular domain: Rotation mechanism for transmembrane signal transduction. *J. Biol. Chem.* **279**, 28625–28631 (2004).
26. F. van den Akker *et al.*, Structure of the dimerized hormone-binding domain of a guanylyl-cyclase-coupled receptor. *Nature* **406**, 101–104 (2000).
27. H. H. Chen *et al.*, Novel protein therapeutics for systolic heart failure: Chronic subcutaneous B-type natriuretic peptide. *J. Am. Coll. Cardiol.* **60**, 2305–2312 (2012).
28. Y. Chen *et al.*, CRRL269: A novel designer and renal-enhancing pGC-A peptide activator. *Am. J. Physiol. Regul. Integr. Comp. Physiol.* **314**, R407–R414 (2018).
29. Y. Chen *et al.*, C53: A novel particulate guanylyl cyclase B receptor activator that has sustained activity in vivo with anti-fibrotic actions in human cardiac and renal fibroblasts. *J. Mol. Cell. Cardiol.* **130**, 140–150 (2019).
30. A. E. Kennedy *et al.*, A surface plasmon resonance spectroscopy method for characterizing small-molecule binding to nerve growth factor. *J. Biomol. Screen.* **21**, 96–100 (2016).
31. S. H. Reginald *et al.*, Differential regulation of ANP and BNP in acute decompensated heart failure: Deficiency of ANP. *JACC Heart Fail.* **7**, 891–898 (2019).
32. C. M. Ferrario *et al.*, Angiotensin (1-12) in humans with normal blood pressure and primary hypertension. *Hypertension* **77**, 882–890 (2021).
33. J. C. Burnett Jr. *et al.*, Atrial natriuretic peptide elevation in congestive heart failure in the human. *Science* **231**, 1145–1147 (1986).